ORIGINAL ARTICLE

lajss.org© Latin American Journal of Solids and Structures

www.lajss.org

Analysis of Internal Resonance of a 3DOF Dynamic System Reduced from the Tower-Cable-Beam Structure

Kefan Chen[a], Yuan Li[a,b*], Kang Wang[a]

[a] School of Highway, Chang'an University–CHD, Xi'an 710064, China. Email: kfchen@chd.edu.cn, 2020221005@chd.edu.cn
[b] Key laboratory of Old Bridge Detection and Reinforcement Technology of Ministry of Transport, Chang'an University–CHD, Xi'an 710064, China. Email: liyuan@chd.edu.cn

* Corresponding author

https://doi.org/10.1590/1679-78257029

Abstract

To study the complex mechanism of the high-dimensional nonlinear cable systems, a 3 degree-of-freedom model reduced from the tower-cable-beam structure is proposed and investigated in this paper. Based on the D'Alembert Principle, the dynamic equations of in-plane and out-of-plane vibration are established and simulated by the 4th-order Runge-Kutta method. The results exhibit the phenomenon of coupling internal resonance under the systematical conditions revealed by the analytical analysis on the dynamic equations. The smaller mass ratio of the cable-beam would lead to a greater vibration intensity while the tensile stiffness and initial force of the cable have no significant effect. The in-plane and out-plane cable vibrations are independent, and the internal resonance would not be excited by the harmonic excitation in the cable axis. Additionally, applying damping on any component of the system is verified to be an effective approach to vibration reduction. Compared with ordinary cables, cables with less-weight and high-strength materials would be exited to less vibration intensity under the same external excitation.

Keywords

Bridge engineering, internal resonance, in-plane vibration, out-of-plane vibration, analytical simulation

Graphical abstract

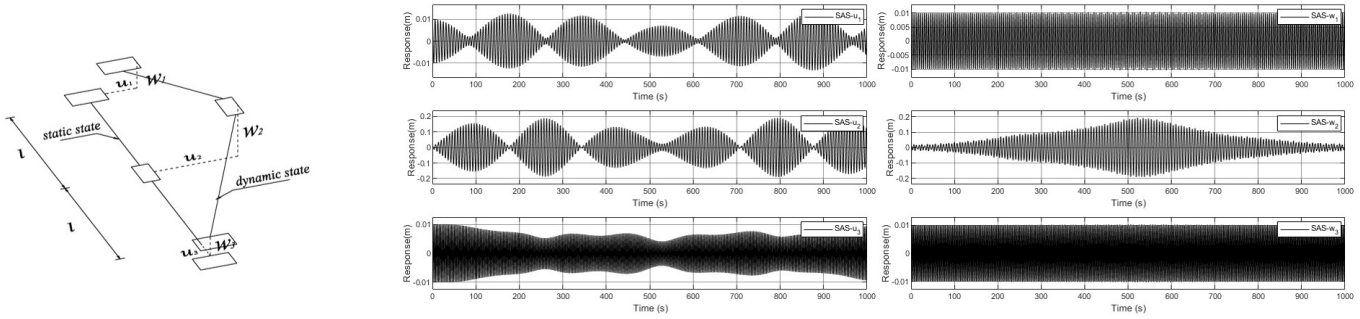

Received: March 09, 2022; In Revised Form: April 06, 2022; Accepted: April 12, 2022; Available online: April 14, 2022
https://doi.org/10.1590/1679-78257029

1 INTRODUCTION

Cable coupled systems are widely used for loading-carrying structures, such as stayed bridges, suspended roofs, and the construction process of arch bridges. The characteristics of high flexibility and low damping promote the system to obtain more favored by engineering applications. However, the non-linear behaviors of the system are easily subjected to potentially damaging amplitude motion or fatigue failure of the cable and provide a high risk of safe operation (Ming H W, Yi Q X, Hai T L, et al., 2014). It has been widely observed in engineering practice that severe oscillations of the cables are excited under no wind or low load of the vehicles (Main, J. A., and Jones, N. P., 1999) (Tabatabai, Habib, and Armin B. Mehrabi, 1999).

To further study the phenomena of the internal resonance in cable-stayed bridges, Benedettini studied the dynamics of finite forced structures with quadratic and cubic nonlinearities in the dynamic equations of cable-stayed bridges (Benedettini F, Rega G, 1987). Fujino established a simple model reduced from a cable-beam composite structure by combining experiments and theoretical analysis and observed the resonance phenomenon of '1:2' cable-beam parametric resonance motion (Fujino Y, Warnitchai P, and Pacheco B M, 1993). Virlogeux M (1998) first reduced the components to concentrated masses and study the mechanism of the resonance. In line with this, Zhan and Zhong (1998) and Zhang, Wang and Yang (2010) derived the dynamic equations of the cable-beam system based on the D'Alembert principle and explained the relationship between the natural frequency of each component and the global frequency of the dynamic system. In line with this solution method, the researchers derived the ordinary differential equations (ODEs) of variable cable structure models through the non-linear boundary conditions of the structure and systematically analyzed the influence factors (Yu Yanlei, Gao WeiCheng, and Sun Yi, 2010) (S. S. Chen and B. N. Sun, 2003) (Zhang L N, Li F C, Wang X Y, et al., 2017). Moreover, Georgakis et al. (2013) (2005) studied the extensive vibration behavior caused by the plane structure vibration of cable-stayed bridge systems and investigated the vibrations control methods from the perspective of material properties. Wang, Zhang, et al. (2018) proposed a parameterized vibration model of stayed cable under the combination of gradient temperature field and bridge deck stimulation to study the ultra-long cable-stayed in a non-uniform temperature field and bridge.

These research results all revealed that the ratios between the natural frequency with other different components (RNF) take an important role in the excitation of internal resonance. And the resonance is excited by the high-order polynomial coefficients of the dynamic equations, which require thousands of finite elements to simulate the complex vibration mechanism of the cable structures (G. Ricciardi and F. Saitta, 2008). To address this problem and analyze the mechanism of global-resonance motion, a few researchers developed new finite elements of cable or other components and analyzed the sensitives of the influence factors through the Variables Separation Method (Gattulli V, Lepidi M, 2003) (Wu Z, Wei J, 2019). Additionally, Caetano (E. Caetano and A. Cunha, 2008), Ouni (M. H. El Ouni and N. Ben Kahla, 2012) and Sun (C. Sun and Y. Zhao, 2018) et.al studied the mutual coupling process of each mode through segmental analysis and phase-free filtering through the field test or experiments. It was found that forced vibration, local-mixed mode coupled vibration, and the simultaneous occurrence of combined internal resonance was the root cause that the single-frequency external stimulation could stimulate the stay cable.

However, it is known that the use of 3D FE modeling in these cases is not practical and that conventional beam models do not solve properly the problem. Additionally, due to the lack of high-effectiveness of the solving methods for high-dimensional nonlinear systems, the nonlinear dynamic behavior of the integral cable-stayed bridge is quite complicated, and in-depth research is facing great difficulties (H. J. Kang, T. D. Guo, and Y. Y. Zhao, 2016). Studies on the vibration characteristics of multi-degree-of-freedom parametric resonance systems are more in line with the engineering practice, and the research results can lay a foundation for further expanding the research in this field or guiding the construction.

Laying on the foundation of literature (Virlogeux M, 1998) (Kefan Chen and Shuanhai He, 2021) (K. Zhan and W. X. Zhong, 1998) (Y. Zhang and H. Wang, 2010), this paper systematically investigates and discusses the characteristics and influencing factors of the 3DOF freedom coupling resonance system of the tower-cable-beam. The simulation results through the 4th-order Runge-Kutta method, which is further illustrated the effectiveness through the verification of comparison with the finite element method (FEM), are helpful in the related discussion of the coupled characteristic and influence factor sensitives. Through the model and method proposed in this study, the possibility of parametric resonance in the dynamic system can be easily and quickly estimated compared to other models coupling nonlinear cables and the 3D finite element model of the bridge having thousands of elements.

2 THE REDUCED DYNAMIC MODEL AND THE ANALYTICAL ANALYSIS

2.1 The reduced dynamic model and the mathematical expression

Along with the reduced idea proposed in the literature (Virlogeux M, 1998), the tower, cable, and beam are reduced into the lumper mass blocks, respectively, as shown in Figure 1(a). It is assumed that the effect of the gravity of the cable or the tower on the transverse direction is ignorable. Additionally, the subscripted 1, 2, 3 represent the tower, the cable, and the beam, respectively; the subscripted 'u' and 'w' represents the in-plane vibration and out-of-plane vibration, respectively. The tower, assumed to vibrate only in the transverse direction due to the tension of the cable, is reduced into a lumped mass block m_1 with the air damping c_{u1} and c_{w1}. The springs k_{u1} and k_{w1} are set to simulate the in-plane and out-of-plane bending stiffness of the tower. The cable is assumed to vibrate only in the transverse direction due to the instantaneous tension of both sides (T_1 and T_2, while T_0 is the tension at the initial state of equilibrium), is reduced into a lumped mass block m_2 with the air damping c_{u2} and c_{w2}. The Euler-Bernoulli beam, assumed to vibrate only in the axial direction of the cable, is reduced into a lumped mass block m_3 with the air damping c_{u3} and c_{w3}. The transverse springs k_3 and k_{w3} are set to simulate the in-plane and out-of-plane bending stiffness of the beam, respectively. It is also assumed that the initial state of the system is in equilibrium, while two massless strings of the same length l are connected with cable to tower and cable to beam. When the resonance is occurring, the angle between the ends of the cable to beam or that of cable to tower of in-plane vibration are set as α_1 and α_2 while β_1 and β_2 are set for the out-of-plane vibration, respectively. The vibration displacement of the tower relative to the equilibrium position in these two planes are u_1 and w_1; the vibration displacement of the cable relative to the equilibrium position in these two planes are u_2 and w_2; the vibration displacement of the beam relative to the equilibrium position in these two planes are u_3 and w_3. The dynamic state line of the dynamic system is shown in Figure 1(b).

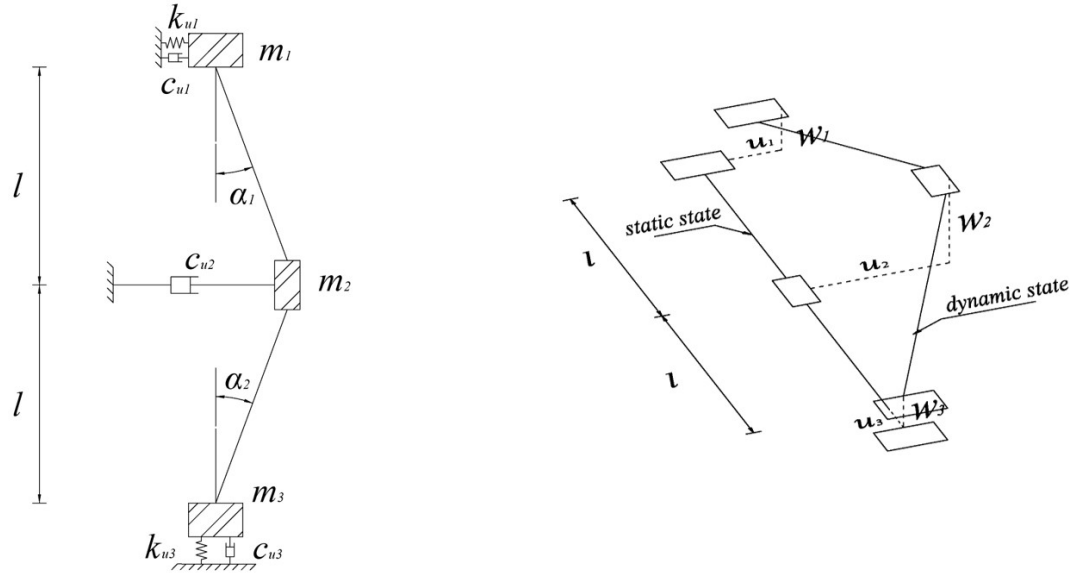

***(a)** in-plane vibration* ***(b)** out-of-plane vibration*

Figure 1 The three-degree-of-freedom model reduced from the tower-cable-beam dynamic system: (a) in-plane vibration; (b) out-of-plane vibration.

According to the D'Alembert Principle, the vibration equations of the model in Figure 1 can be obtained as follows.

$$-m_1\ddot{u}_1 = k_{u1}u_1 + c_{u1}\dot{u}_1 - T_1 \cos\beta_1 \sin\alpha_1 - \psi_{u1}\cos\omega_{u1}t \tag{1}$$

$$-m_1\ddot{w}_1 = k_{w1}w_1 + c_{w1}\dot{w}_1 - T_1 \sin\beta_1 - \psi_{w1}\cos\omega_{w1}t \tag{2}$$

$$-m_2\ddot{u}_2 = c_{w2}\dot{u}_2 + T_1 \cos\beta_1 \sin\alpha_1 + T_2 \cos\beta_2 \sin\alpha_2 - \psi_{u2}\cos\omega_{u2}t \tag{3}$$

$$-m_2\ddot{w}_2 = c_{w2}\dot{w}_2 + T_1 \sin\beta_1 + T_2 \sin\beta_2 - \psi_{w2}\cos\omega_{w2}t \tag{4}$$

$$-m_3\ddot{u}_3 = k_{u3}u_3 + c_{w3}\dot{u}_3 + T_2\cos\beta_2\cos\alpha_2 - m_3 g - \psi_{u3}\cos\omega_{u3}t \tag{5}$$

$$-m_3\ddot{w}_3 = k_{w3}w_3 + c_{w3}\dot{w}_3 + T_2\sin\beta_2 - \psi_{w3}\cos\omega_{w3}t \tag{6}$$

where g represents the acceleration of gravity; ψ is the amplitude of the external excitation on the component; ω is the frequency of the external excitation on the component. As seen in Figure 1, the boundary conditions of the dynamic system can be obtained:

$$l_1{}^2 = l^2 + (u_2 - u_1)^2 + (w_2 - w_1)^2 = (l + \Delta l_1)^2 \tag{7}$$

$$l_2{}^2 = (u_3 + l)^2 + u_2{}^2 + (w_3 - w_1)^2 = (l + \Delta l_2)^2 \tag{8}$$

After ignoring higher-order epsilons, the dynamic tensile force of the cable can be obtained:

$$\Delta T_1 = EA \cdot \frac{(u_2-u_1)^2+(w_2-w_1)^2}{2l^2} \tag{9}$$

$$\Delta T_2 = EA \cdot \frac{u_2{}^2+u_3{}^2+2u_3 l+(w_3-w_2)^2}{2l^2} \tag{10}$$

Additionally, it is assumed by the theory of large displacement, the simplifications can be obtained:

$$\sin\alpha_1 = \frac{u_2-u_1}{\sqrt{l^2+(u_2-u_1)^2}} \approx \frac{u_2-u_1}{l}, \cos\alpha_1 = \frac{l}{\sqrt{l^2+(u_2-u_1)^2}} \approx 1 \tag{11}$$

$$\sin\alpha_2 = \frac{u_2}{\sqrt{(l+u_3)^2+u_2{}^2}} \approx \frac{u_2}{l}, \cos\alpha_2 = \frac{l}{\sqrt{(l+u_3)^2+u_2{}^2}} \approx 1 \tag{12}$$

$$\sin\beta_1 = \frac{w_2-w_1}{l_1} \approx \frac{w_2-w_1}{l}, \cos\beta_1 = \frac{\sqrt{l_1{}^2-(w_2-w_1)^2}}{l_1} \approx 1 \tag{13}$$

$$\sin\beta_2 = \frac{-w_3+w_2}{l_2} \approx \frac{-w_3+w_2}{l}, \cos\beta_2 = \frac{\sqrt{l_2{}^2-(w_3-w_2)^2}}{l_2} \approx 1 \tag{14}$$

By subsisting Eq. (11) ~ Eq. (14) into Eq. (1) ~ Eq. (6), the in-plane and out-of-plane dynamic equations of the three-degree-of-freedom system can be derived and reduced as follows (Virlogeux M, 1998):

$$\ddot{u}_1 + \kappa_{u1}{}^2\cdot u_1 + \dot{c}_{u1}\cdot\dot{u}_1 + \Gamma_{1,1}\cdot u_1{}^3 + \Gamma_{1,2}\cdot u_2 + \Gamma_{1,3}\cdot u_1{}^2u_2 + \Gamma_{1,4}\cdot u_1u_2{}^2 + \Gamma_{1,5}\cdot u_2{}^3 + \Gamma_{1,6}\cdot u_1w_1{}^2 + \Gamma_{1,7}\cdot u_2w_1{}^2 + \Gamma_{1,8}\cdot u_1w_1w_2 + \Gamma_{1,9}\cdot u_2w_1w_2 + \Gamma_{1,10}\cdot u_1w_2{}^2 + \Gamma_{1,11}\cdot u_2w_2{}^2 = \Psi_{u1}\cos\omega_{u1}t \tag{15}$$

$$\ddot{w}_1 + \kappa_{w1}{}^2\cdot w_1 + \dot{c}_{w1}\cdot\dot{w}_1 + \Pi_{1,1}\cdot u_1{}^2w_1 + \Pi_{1,2}\cdot u_1u_2w_1 + \Pi_{1,3}\cdot u_2{}^2w_1 + \Pi_{1,4}\cdot w_1{}^3 + \Pi_{1,5}\cdot w_2 + \Pi_{1,6}\cdot u_1{}^2w_2 + \Pi_{1,7}\cdot u_1u_2w_2 + \Pi_{1,8}\cdot u_2{}^2w_2 + \Pi_{1,9}\cdot w_1{}^2w_2 + \Pi_{1,10}\cdot w_1w_2{}^2 + \Pi_{1,11}\cdot w_2{}^3 = \Psi_{w1}\cos\omega_{w1}t \tag{16}$$

$$\ddot{u}_2 + \kappa_{u2}{}^2\cdot u_2 + \dot{c}_{u2}\cdot\dot{x}_2 + \Gamma_{2,1}\cdot u_1 + \Gamma_{2,2}\cdot u_1{}^3 + \Gamma_{2,3}\cdot u_1{}^2u_2 + \Gamma_{2,4}\cdot u_1u_2{}^2 + \Gamma_{2,5}\cdot u_2{}^3 + \Gamma_{2,6}\cdot u_2u_3 + \Gamma_{2,7}\cdot u_2u_3{}^2 + \Gamma_{2,8}\cdot u_1w_1{}^2 + \Gamma_{2,9}\cdot u_2w_1{}^2 + \Gamma_{2,10}\cdot u_1w_1w_2 + \Gamma_{2,11}\cdot u_2w_1w_2 + \Gamma_{2,12}\cdot u_1w_2{}^2 + \Gamma_{2,13}\cdot u_2w_2{}^2 + \Gamma_{2,14}\cdot u_2w_2w_3 + \Gamma_{2,15}\cdot u_2w_3{}^2 = \Psi_{u2}\cos\omega_{u2}t \tag{17}$$

$$\ddot{w}_2 + \kappa_{w2}{}^2\cdot w_2 + \dot{c}_{w2}\cdot\dot{w}_2 + \Pi_{2,1}\cdot w_1 + \Pi_{2,2}\cdot u_1{}^2w_1 + \Pi_{2,3}\cdot u_1u_2w_1 + \Pi_{2,4}\cdot u_2{}^2w_1 + \Pi_{2,5}\cdot w_1{}^3 + \Pi_{2,6}\cdot u_1{}^2w_2 + \Pi_{2,7}\cdot u_1u_2w_2 + \Pi_{2,8}\cdot u_2{}^2w_2 + \Pi_{2,9}\cdot u_3w_2 + \Pi_{2,10}\cdot u_3{}^2w_2 + \Pi_{2,11}\cdot w_1{}^2w_2 + \Pi_{2,12}\cdot w_1w_2{}^2 + \Pi_{2,13}\cdot w_2{}^3 + \Pi_{2,14}\cdot w_3 + \Pi_{2,15}\cdot u_3{}^2w_3 + \Pi_{2,16}\cdot u_3w_3 + \Pi_{2,17}\cdot u_3{}^2w_3 + \Pi_{2,18}\cdot w_2{}^2w_3 + \Pi_{2,19}\cdot w_2w_3{}^2 + \Pi_{2,20}\cdot w_3{}^3 = \Psi_{w3}\cos\omega_{w3}t \tag{18}$$

$$\ddot{u}_3 + \kappa_{u3}{}^2\cdot u_3 + \dot{c}_{u3}\dot{u}_3 + \Gamma_{3,1}\cdot u_2{}^2 + \Gamma_{3,2}\cdot u_3{}^2 + \Gamma_{3,3}\cdot w_2{}^2 + \Gamma_{3,4}\cdot w_2w_3 + \Gamma_{3,5}\cdot w_3{}^2 = \Psi_{u3}\cos\omega_{u3}t \tag{19}$$

$$\ddot{w}_3 + {\kappa_{w3}}^2 \cdot w_3 + \dot{c}_{w3} \cdot \dot{w}_3 + \Pi_{3,1} \cdot w_2 + \Pi_{3,2} \cdot {u_2}^2 w_2 + \Pi_{3,3} \cdot u_3 w_2 + \Pi_{3,4} \cdot {u_3}^2 w_2 + \Pi_{3,5} \cdot {w_2}^3 + \Pi_{3,6} \cdot {u_2}^2 w_3 + \Pi_{3,7} \cdot u_3 w_3 + \Pi_{3,8} \cdot {u_3}^2 w_3 + \Pi_{3,9} \cdot {w_2}^2 w_3 + \Pi_{3,10} \cdot w_2 {w_3}^2 + \Pi_{3,11} {w_3}^3 = \Psi_{w3} \cos \omega_{w3} t \quad (20)$$

It is important that the global vibration of the structure presents the global mode frequency and the corresponding mode shape. On this basis, the κ does not symbol the global frequency of the structure, resulting in that κ is introduced as the dynamic parameter of each component here in this paper. The dynamic parameters have a certain relationship with the global resonance to local resonance, whose dimensions are equivalent to frequency (Fujino Y, Warnitchai P, and Pacheco B M, 1993) (M. H. El Ouni, N. Ben Kahla, and A. Preumont, 2012). As shown in Figure 1(a), if the tower, cable, or the beam are regarded as a discrete vibration system excited by the external forces, they all have an independent natural frequency and the related mode shape. Thus, κ is known as the frequency of the local mode in some publications (Gattulli V, Lepidi M, 2003) (K. Zhan and W. X. Zhong, 1998) (Y. Zhang and H. Wang, 2010). The detailed coefficients can be obtained in Appendix 1.

2.2 The analytical analysis

The Multi-Scale Method is widely applied for the solution of the ODEs (C. Sun and Y. Zhao, 2018) (H. J. Kang, T. D. Guo, and Y. Y. Zhao, 2016). To solute the ODEs of the dynamic system, as shown in Eq. (1) ~ Eq. (6), a small bookkeeping parameter ε is introduced into the solution of each variable, as shown as follows:

$$\varepsilon^n \lambda_{jn}(t_0, t_1), \quad x_j = \sum_{n=1}^{2} \quad (21)$$

wheret_0, t_1 represents the multi-scale of the time ($t_n = \varepsilon^n \cdot \tau, n \in [0,1]$); λ_{jn}represents the function under different time scale variables (t_0 and t_1) ($\lambda = u, w$). Substituting Eq. (21) into Eq. (1) ~ Eq. (6) and equating the coefficient of the same power of ε to be zero, the differential equations can be obtained:

ε^1:

$${D_0}^2 u_{11} + {k_{u1}}^2 u_{11} + \Gamma_{1,2} u_{21} = 0 \quad (22)$$

$${D_0}^2 w_{11} + {k_{w1}}^2 w_{11} + \Pi_{1,5} w_{21} = 0 \quad (23)$$

$${D_0}^2 u_{21} + {k_{u2}}^2 u_{21} + \Gamma_{2,1} u_{11} = 0 \quad (24)$$

$${D_0}^2 w_{21} + {k_{w2}}^2 w_{21} + \Pi_{2,1} w_{11} + \Pi_{2,14} w_{31} = 0 \quad (25)$$

$${D_0}^2 u_{31} + {k_{u3}}^2 u_{31} = 0 \quad (26)$$

$${D_0}^2 w_{31} + {k_{w3}}^2 w_{31} + \Pi_{3,1} w_{21} = 0 \quad (27)$$

ε^2:

$${D_0}^2 u_{12} + {k_{u1}}^2 u_{12} = -\Gamma_{1,2} u_{22} - 2 D_0 D_1 u_{11} \quad (28)$$

$${D_0}^2 w_{12} + {k_{w1}}^2 w_{12} = -\Pi_{1,5} w_{22} - 2 D_0 D_1 w_{11} \quad (29)$$

$${D_0}^2 u_{22} + {k_{u2}}^2 u_{22} = -\Gamma_{2,1} u_{12} - \Gamma_{2,6} u_{21} u_{31} - 2 D_0 D_1 u_{21} \quad (30)$$

$${D_0}^2 w_{22} + {k_{w2}}^2 w_{22} = -\Pi_{2,1} w_{12} - \Pi_{2,9} u_{31} w_{21} - \Pi_{2,14} w_{32} - \Pi_{2,16} u_{31} w_{31} - 2 D_0 D_1 w_{21} \quad (31)$$

$${D_0}^2 u_{32} + {k_{u3}}^2 u_{32} = -\Gamma_{3,1} {u_{21}}^2 - \Gamma_{3,2} {u_{31}}^2 - \Gamma_{3,3} {w_{21}}^2 - \Gamma_{3,4} w_{21} w_{31} - \Gamma_{3,5} {w_{31}}^2 - 2 D_0 D_1 u_{31} \quad (32)$$

$${D_0}^2 w_{32} + {k_{w3}}^2 w_{32} = -\Pi_{3,1} w_{22} - \Pi_{3,3} u_{31} w_{21} - \Pi_{3,7} u_{31} w_{31} - 2 D_0 D_1 w_{31} \quad (33)$$

where $D_n = \partial/\partial t_0, n \in [0,1]$. From Eq. (15) ~ Eq. (20) , the 1st order of ε of the cable and the tower exists an extra polynomial $\Gamma_{1,2}u_{21}$、$\Pi_{1,5}w_{21}$、$\Gamma_{2,1}u_{11}$、$\Pi_{2,1}w_{11} + \Pi_{2,14}w_{31}$、$\Pi_{3,1}w_{21}$, respectively. It is illustrated that the coupling term of the cable exists in the dynamic equation that expresses the tower participating in the resonance process. The polynomials are obtained only in the tower-cable coupling system where two resonances of two different components in the same direction is occurring. Further, the general solutions of Eq. (22) and Eq. (28) have the following forms:

$$u_{11} = A_{u_1}(t_1, t_2)e^{ik_{u1}t_0} + c.c. \tag{34}$$

$$u_{21} = A_{u_2}(t_1, t_2)e^{ik_{u2}t_0} + c.c. \tag{35}$$

$$u_{31} = A_{u_3}(t_1, t_2)e^{ik_{u3}t_0} + c.c. \tag{36}$$

$$w_{11} = A_{w1}(t_1, t_2)e^{ik_{w1}t_0} + c.c. \tag{37}$$

$$w_{21} = A_{w2}(t_1, t_2)e^{ik_{w2}t_0} + c.c. \tag{38}$$

$$w_{31} = A_{w3}(t_1, t_2)e^{ik_{w3}t_0} + c.c. \tag{39}$$

where c.c. represents the complex conjugate of the preceding terms; $A_n\,(t_1, t_2)$ represents the unknown complex functions of the time scale of t_1, which is also known with a polar form as:

$$A_{un}(t_1, t_2) = \frac{1}{2}\zeta_{un}(t_1, t_2)e^{i\theta_{un}(t_1,t_2)} \tag{40}$$

$$A_{wn}(t_1, t_2) = \frac{1}{2}\zeta_{wn}(t_1, t_2)e^{i\theta_{wn}(t_1,t_2)} \tag{41}$$

where $\zeta_n(t_1, t_2)$ and $\theta_n(t_1, t_2)$ represents the amplitude and the phase angle of $A_n\,(t_1, t_2)$. Based on the related theory of the quadratic constant-coefficient non-homogeneous linear differential equation, through the analysis of the duration term, the parametric resonance conditions of the dynamic system can be obtained as follows:

$$k_{u1} = k_{u2} \tag{42}$$

$$k_{w_1} = k_{w2} \tag{43}$$

$$k_{u3} = 2k_{u2} \tag{44}$$

$$k_{u3} = 2k_{w2} \tag{45}$$

$$k_{w2} = k_{w3} \tag{46}$$

$$k_{u3} = 2k_{u1} \tag{47}$$

$$2k_{w3} = k_{u2} \tag{48}$$

$$k_{u3} = 2k_{w3} \tag{49}$$

$$k_{u3} = k_{w2} + k_{w3} \tag{50}$$

$$k_{w2} = k_{u3} + k_{w3} \tag{51}$$

$$k_{w2} = k_{u3} + k_{w3} \tag{52}$$

Once the above conditions were satisfied, the coefficient term, such as $t_0 e^{i\kappa_{u1} t_0}$, $t_0 e^{-i\kappa_{u1} t_0}$ and et.al, would be observed in the solutions of Eq. (22) ~ Eq. (27) and Eq. (28) ~ Eq. (33), where the severe internal resonance would be observed in the time history of the cable of in-plane or the out-of-plane. Most scholars generally paid more attention to the condition of Eq. (42) ~ Eq. (49). In fact, it is ignored that the sum relationship of the in-plane and out-of-plane modes are also the critical factors that cause the resonance. Thus, such a phenomenon has also been found in several studies of the model test (C. Sun, Y. Zhao, J. Peng, et al., 2018) (SUN C.S., Zhao Y.B., Kang H.J., Zhao Y.Y.,2018b) while no further discussions have been made through the model test of a complex internal resonance system.

3 CASE STUDY

3.1 Modal analysis

From Eq. (15) ~ Eq. (20), the eigenfunction can be obtained as follow:

$$\boldsymbol{m}_i \cdot \begin{bmatrix} \ddot{\boldsymbol{u}}_i & \\ & \ddot{\boldsymbol{w}}_i \end{bmatrix} + \boldsymbol{k}_i \cdot \begin{bmatrix} \boldsymbol{u}_i & \\ & \boldsymbol{w}_i \end{bmatrix} = 0 \tag{53}$$

where i=1,2,3. On this basis, the eigenmatrix G can be obtained as follows:

$$\boldsymbol{G} = \boldsymbol{m}_i{}^{-1} \cdot \boldsymbol{k}_i = \begin{bmatrix} \kappa_{u1}{}^2 & & & & & \\ & \kappa_{u2}{}^2 & & & & \\ & & \kappa_{u3}{}^2 & & & \\ & & & \kappa_{w1}{}^2 & & \\ & & & & \kappa_{w2}{}^2 & \\ & & & & & \kappa_{w3}{}^2 \end{bmatrix} \tag{54}$$

By solving the Eigen roots of the above matrix, the vibration frequency of the system ω_n can be obtained. On this basis, after synthesizing the Refs. (Benedettini F, Rega G, 1987) (Fujino Y, Warnitchai P, and Pacheco B M, 1993), the fundamental parameters of the components are presented in Table 1, also named CC1 in the following research.

Table 1. The basic parameters of different components (CC1)

m1(kg)	μm2(kg)	m3(kg)	l(m)	T0(N)
2000	0.5	800	20	100
EA(N)	ku1(N/m)	ku3(N/m)	kw1(N/m)	kw3(N/m)
16000	2000	2400	4000	4000

Considering the nonlinear geometry of the system, with the integral method of Newmark-β and the average step of 0.02s, a finite element model of the system is established to devote a modal analysis. The calculated results of modes frequencies and mode shapes are presented in Table 2 and Figure 2, respectively.

Table 2. The mode properties of the dynamic system

Natural frequency	Mode No.	FEM (rad/s)	Analytical (rad/s)	Error (%)
In-plane	1	0.9820	1.0000	1.80
	2	1.0174	1.0013	1.60
	3	1.9990	2.0000	0.50
Out-of-plane	1	0.9980	1.0000	0.20
	2	1.4148	1.4151	0.02
	3	2.2365	2.2347	0.08

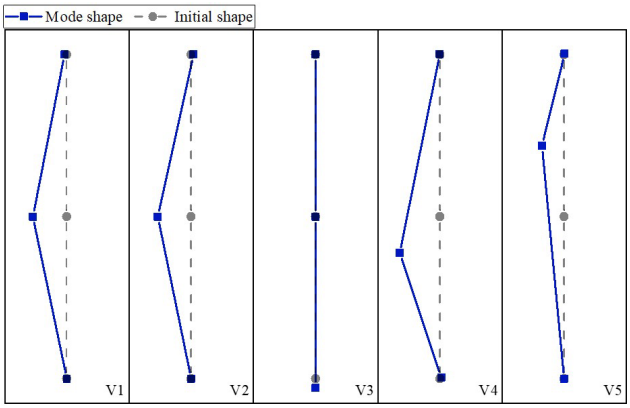

Figure 2 The in-plane mode shapes of the system

It is noticeable that the first three orders of the model are similar to the natural frequencies of these three components. It illustrates that the natural vibration shapes and frequencies of these three components occupy the lower-order modes of the system, respectively. It can be also concluded from the first three mode shapes of the system in Figure 2.

3.2 Analytical simulation and verification

The powerful combination of SIMULINK/MATLAB software has always been regarded as an effective simulation tool that is used to simplify the methods of solving differential equations (Menwer Attarakih, Mazen Abu-Khader, and Hans-Jörg Bart, 2013). Based on the 4th Runge-Kutta Method (symboled as SAS in the following investigation), the time response analysis of the system is applied and the vibration response of the tower, the cable, and the beam can be obtained as follows:

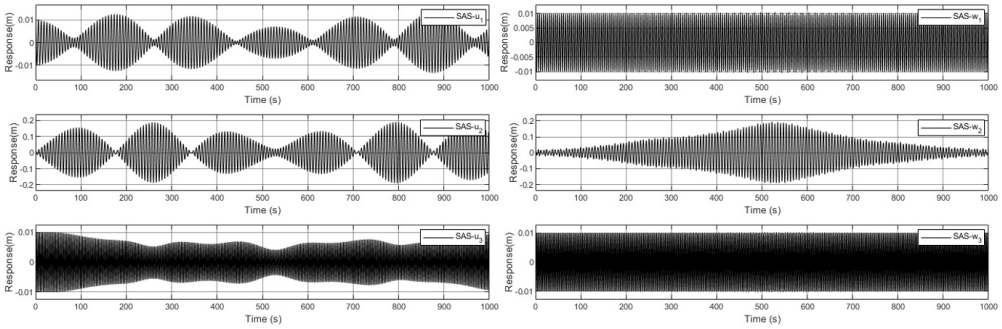

(a)

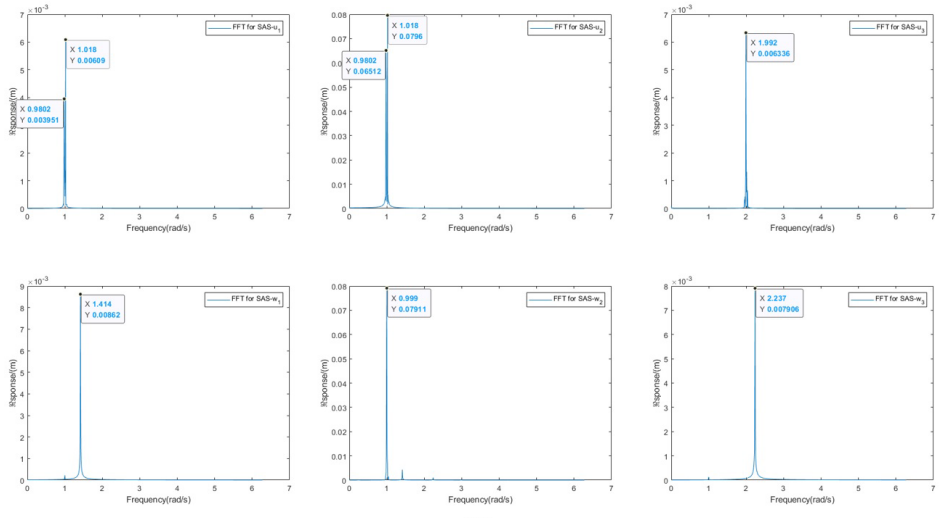

(b)

Figure 3 The vibration analysis of the tower, the cable and the beam: (a) the vibration response of the components; (b) the spectrograms of the components.

From Figure 3, it is illustrated that the coupling internal resonance phenomenon of u1 and w2 can be observed when the local frequency ratio of the cable-beam satisfies 1:2, either is that of the cable-tower satisfies 1:1. It is consistent with the known conclusion. Moreover, it seems that the coupling vibration of the cable in the out-of-plane could be excited by the in-plane motion, which would be further discussed in section 4. To further verify the validity of the derivation process and the reduced model, the time response analysis of the system is proposed through two different methods. One is to propose a time response analysis on the in-plane motion of the cable through the SIMULINK by using the 4th Runge-Kutta Method (SAS-u2); another is analyzed through the finite element method (FEM-u2). And the comparison result is presented in Figure 4.

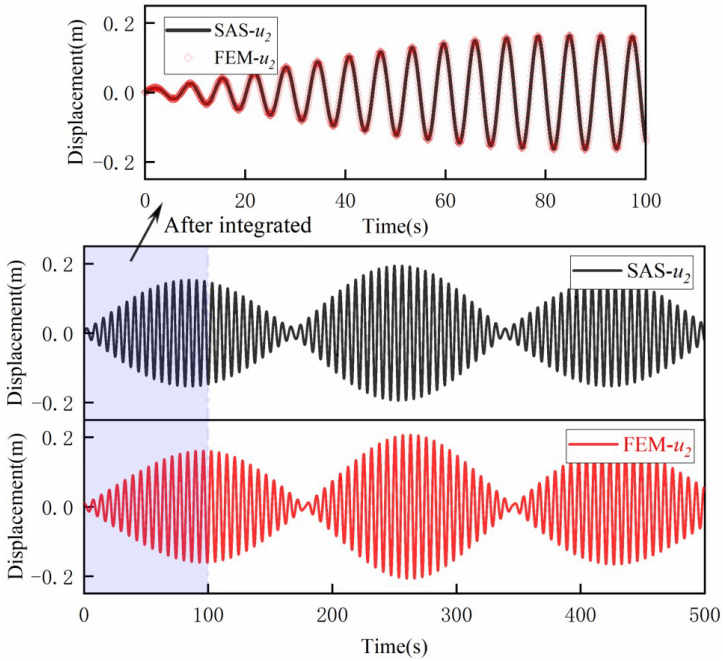

Figure 4 The comparative results of these two methods

In Figure 4, the varying trends of the curves obtained by these two methods stay almost the same, which can be more clearly seen from the integrated figure. It is deeply illustrated that the numerical method of the SIMULINK plays an effective role in solving and simulating the equations.

4 Parametric discussions of the dynamic system

To further discuss the dynamic behaviors, the resonance intensity, symbolled as ε_λ $(\lambda = u, w)$, is introduced to represent the ratio of the maximum response to the initial displacement. To further investigate the ratio condition of the internal resonance, the incremented frequency of the cable's dynamic parameter mode $\sigma_{\lambda 2}$ is also introduced as shown in Eq. (55) and Eq. (56). Additionally, the proximity factors χ_λ and μ_λ are introduced to measure the degree of closeness of the cable's dynamic parameter to the tower's local mode and half of the beam's local mode, respectively, as shown in Eq. (57) and Eq. (58).

$$\Omega_{\lambda 2}{}^{S} = \kappa_{\lambda 2} + \sigma_{\lambda 2}, (\lambda = u, w) \tag{55}$$

$$\Omega_{\lambda 2}{}^{E} = \omega_{\lambda 2} + \sigma_{\lambda 2}, (\lambda = u, w) \tag{56}$$

$$\chi_\lambda = \frac{|\Omega_{\lambda 2}{}^{S} - \kappa_{\lambda 1}|}{\kappa_{\lambda 1}} \tag{57}$$

$$\mu_\lambda = \frac{|\Omega_{\lambda 2}{}^{E} - \kappa_{\lambda 2}|}{\kappa_{\lambda 2}} \tag{58}$$

By changing the value of $\sigma_{\lambda 2}$, the value of dynamic parameter ratio can thus be changed.

4.1 Parametric analysis of the internal resonance

By applying some simple combinations of the parameters, the conditions presented in Eq. (42) ~ Eq. (52) can be verified as shown in Figure 5, with an initial excitation of 0.01m on the component.

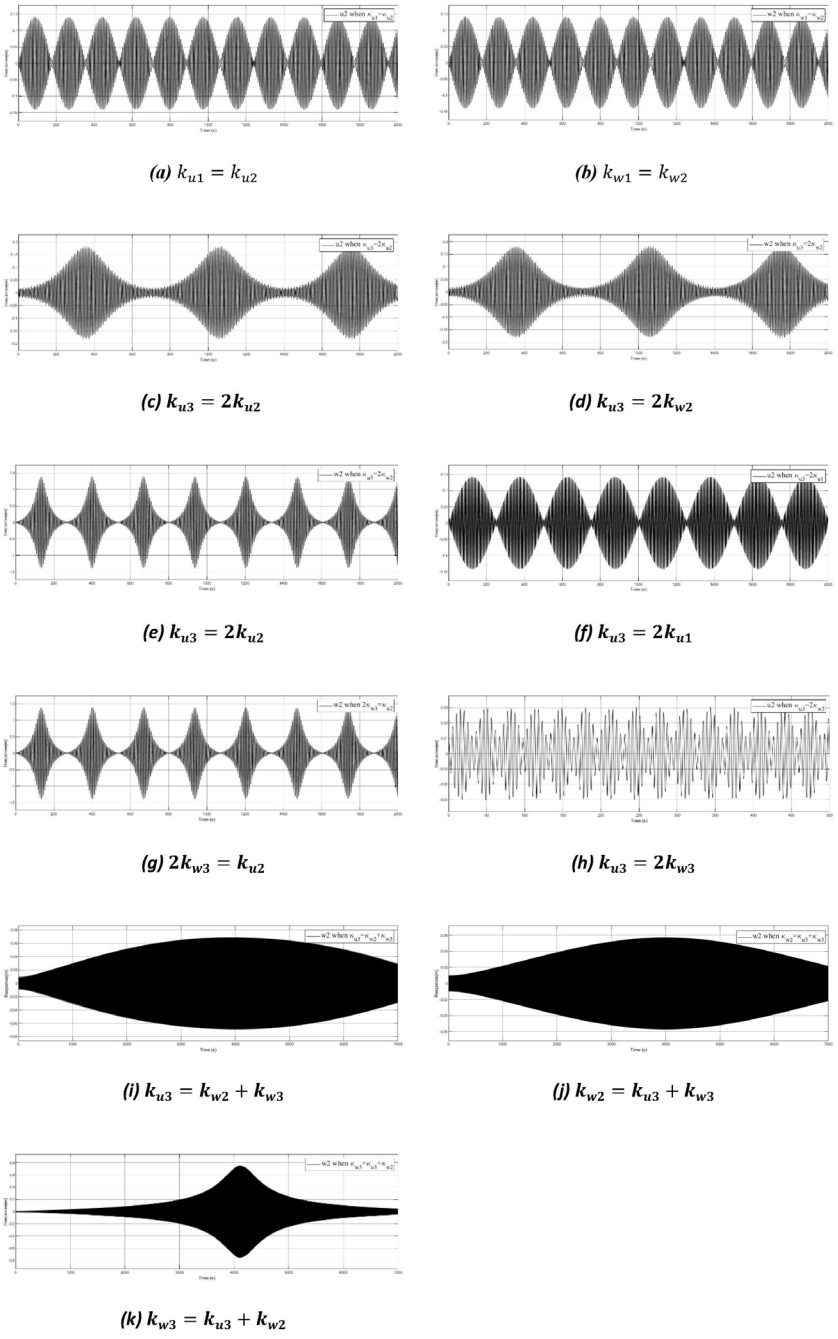

(a) $k_{u1} = k_{u2}$ *(b)* $k_{w1} = k_{w2}$

(c) $\boldsymbol{k_{u3} = 2k_{u2}}$ *(d)* $\boldsymbol{k_{u3} = 2k_{w2}}$

(e) $\boldsymbol{k_{u3} = 2k_{u2}}$ *(f)* $\boldsymbol{k_{u3} = 2k_{u1}}$

(g) $\boldsymbol{2k_{w3} = k_{u2}}$ *(h)* $\boldsymbol{k_{u3} = 2k_{w3}}$

(i) $\boldsymbol{k_{u3} = k_{w2} + k_{w3}}$ *(j)* $\boldsymbol{k_{w2} = k_{u3} + k_{w3}}$

(k) $\boldsymbol{k_{w3} = k_{u3} + k_{w2}}$

Figure 5 The coupling vibration under different conditions

From Figure 5, the coupling vibration, which also exhibits a significant 'beat' character, can be observed on the cable's vibration of in-plane or out-of-plane when the conditions are satisfied. It is interesting that the condition $k_{w3} = 2k_{w2}$ can not lead to the coupling vibration, which is further illustrated that the cable's vibration of the out-of-plane can not be excited to the non-linear vibration by twice the axial frequency in the cable's axial direction. In particular, the factors of the sum relationship (see Eq. (50) ~ Eq. (52)) only lead to the severe resonance in the out-of-plane, as shown in Figure 5(i) ~ Figure 5(k). It is illustrated that the mechanism of the internal resonance becomes more complex when the out-of-plane vibration is considered. In conclusion, the phenomena in Figure 5 also accurately reflect the analytical results in Eq. (42) ~ Eq. (52) are the main factors of the internal resonance in the dynamic system.

As shown in Figure 5, the different characteristics of the cable's vibration can be observed under different conditions. To focus on the investigation of the effect of the basic parameters, such as the ratio of the mass, initial cable force, and EA, on the vibration, the case is applied as follows:

Compared Case 2# (CC2): under the condition of $k_{u1} = k_{u2}$, the basic parameters in Table 1 are also applied here while the following parameters are changed: ku1=4000 N/m, ku3=8000 N/m, kw1=6000 N/m, kw1=10000 N/m. Thus, the ratios of the dynamic parameters are $\kappa_{u1}: \kappa_{u2}: \kappa_{u3} = 1.4: 1: 3.3$ and $\kappa_{w1}: \kappa_{w2}: \kappa_{w3} = 3: 1: 12.5$. On this basis, there is no internal resonance between these two planes.

The method of separation of variables is also applied to investigate the effect of the coefficients on the cable's vibration. On this basis, the variation trend of ε_λ under these conditions can be obtained as shown in Figure 6.

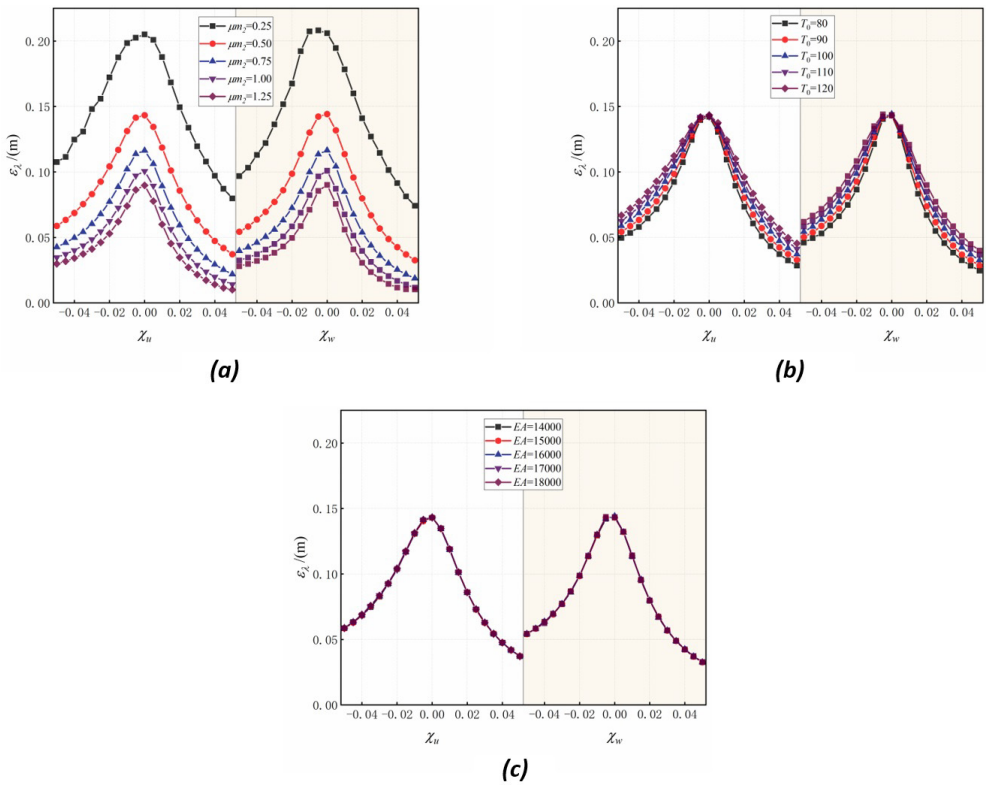

Figure 6 ε_λ under different conditions: (a) with different mass ratio; (b) with different initial cable tension; (c) with different EA.

From Figure 6, when the dynamic system is excited to an initial excitation in the system, the cable would be excited to a severe vibration by a 1:1 indirect excitation in the vertical motion. The response of the cable is maximized at 1:1 while there obviously exists a range of the frequency ratio. Secondly, the variation trends of the in-plane and out-of-plane generally stay inconsistent. Among them, the mass ratio has the most obvious effect on resonance. The smaller the cable mass, the more severe the resonance caused by the same system energy conversion from other components at the cable. It appears to be that a lower initial cable force would minimize the vibration response of the cable while it has little effect at the peak of the response.

4.2 The effect of the external excitation

To further investigate the effect of the excitations from one plane, two conditions which mainly include the in-plane works are first applied in this section.

Compared Case 3-1# (CC3-1): under the condition of $k_{u1} = k_{u2}$, the basic parameters in Table 1 are also applied here while the following parameters are changed: k_{u1}=6000 N/m, k_{u3}=12000 N/m, k_{w1}=6000 N/m, k_{w1}=10000 N/m, $\kappa_{u1}: \kappa_{u2}: \kappa_{u3} = 1.7: 1.7: 4$.

Compared Case 3-2# (CC3-2): under the condition of $k_{u3} = 2k_{u2}$, the basic parameters in Table 1 are also applied here while the following parameters are changed: k_{u1}=4500 N/m, k_{u3}=2400 N/m, k_{w1}=6000 N/m, k_{w1}=10000 N/m, $\kappa_{u1}: \kappa_{u2}: \kappa_{u3} = 1.5: 1: 2$.

On this basis, for clarity and brevity, k_{mi} (i=1,2,3) is introduced to present the correlation coefficients of the effect, which reflects the intensity of each component and is illustrated with a case as shown in Figure 7(a). By applying the

different values of the ω_{ui} on the components, the variation of kmi under different initial conditions are selected as shown in Figure 7(b).

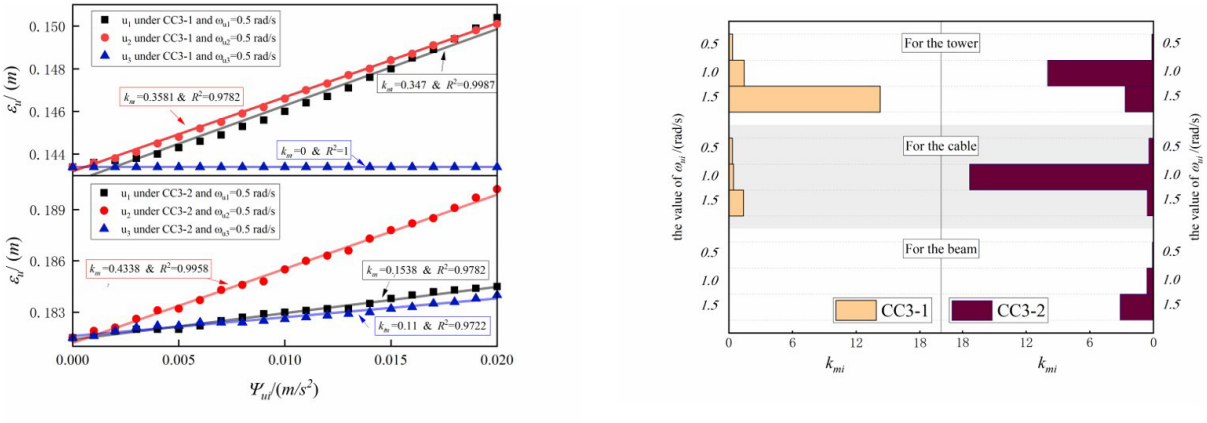

(a) ***(b)***

Figure 7 The variation trend of the parameters with different initial conditions: (a) the trends of ε_u; (b) the trends of k_{mi}.

From Figure 7(a), the correlation coefficients of the fitting $R^2 \in [0.9722,1]$ show a significant relationship of linear increase. The larger the histogram area, the greater the influence intensity, and also the greater the impact on the cable. Under CC3-1, the closer frequency of the external excitation to κ_{u2}, the more obvious the influence of the external excitation amplitude. It can be also observed in the condition of CC3-2 that the intensity of $\omega_{ui} = 1rad/s$ is obviously larger than other values. It can be obtained that the exciting effect of the external excitation is highly consistent with the internal resonance conditions, as shown in Eq. (42) ~ Eq. (52). To further discuss the exciting effect from another plane, the following cases are applied.

Compared Case 4-1# (CC4-1): On the basic parameters of CC2 with no initial displacement applied, the external excitation only from in-plane is applied in this dynamic system, $\omega_{u1} = \kappa_{u1} = \kappa_{u2} = 1rad/s$ with variable Ψ_{u1}.

Compared Case 4-2# (CC4-2): On the basic parameters of CC2 with no initial displacement applied, the external excitation only from out-of-plane is applied in this dynamic system, $\omega_{w1} = \kappa_{u1} = \kappa_{u2} = 1rad/s$ with variable Ψ_{w1}.

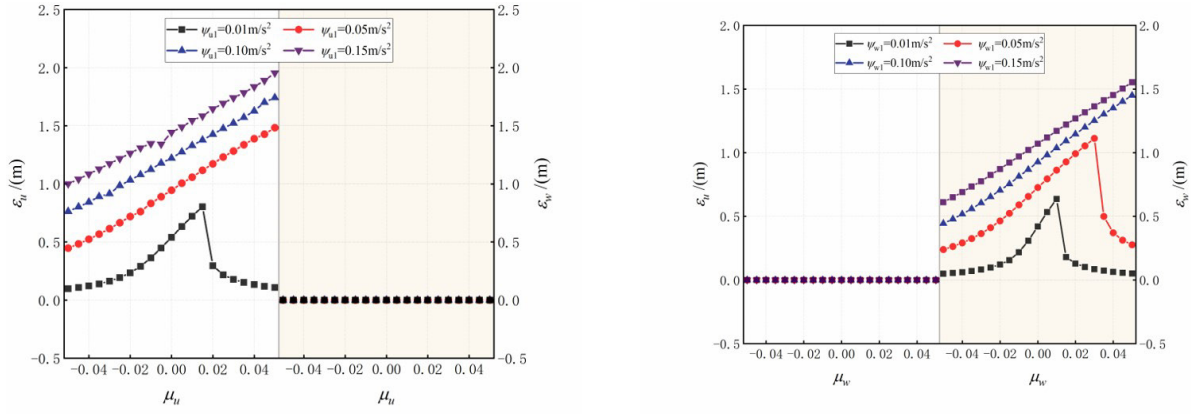

(a) ***(b)***

Figure 8 The variation trends of the parameters with different initial conditions: (a) under CC4-1; (b) under CC4-2.

From Figure 8, it is illustrated that the variation trends of the exciting response in these two planes are the same, while the external vibration seems to be slightly less excited on the numerical value. The excitations of the two planes can not relate to each other and also can not produce the vibration excitation effects on each other. Additionally, the in-plane vibration response of the beam can be produced by a few combined excitations from in-plane and out-of-plane. However, by a number of trial calculations, it can be obtained that the external harmonic excitation in the cable axis (from the beam) can not excite to a severe vibration on the cable. The conclusions also can be drawn that only the out-

of-plane vibration of the cable (w2) can be excited under the conditions of Eq. (50) ~ Eq. (52). The response of the beam of the in-plane can be excited under the conditions of Eq. (50) ~ Eq. (52), while the external excitations in the cable axis can not further excite the in-plane vibration of the cable.

4.3 Discussions of the vibration reduction measure

Vibration control, especially in high-flexibility structures, is always one of the most important goals of the investigations. Structural damping is currently one of the most effective methods for controlling component vibration in civil engineering. Through substituting the parameters in a consistent investigation (Zhang Yan, Wang Huailei, and Yang Jie, 2010), the validity of the method in this paper can be verified by comparing the results in the Ref. (symbolled as RAS) with that of the analytical simulation, as shown in Figure 9.

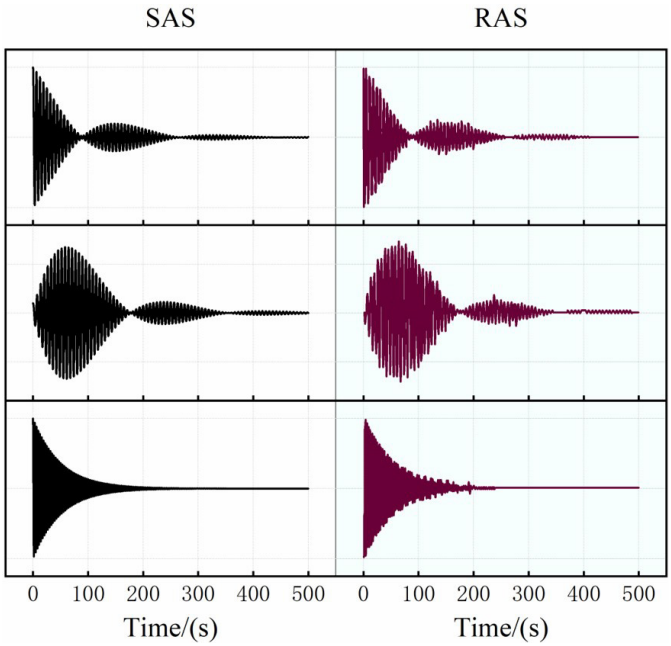

Figure 9 The compared results with the simulation in Ref.

Figure 9 indicates that the reliability and effectiveness of the proposed method in this paper are well-simulated considering the effect of the damping. On this basis, the response of the cable with different damping is selected as shown in Figure 10.

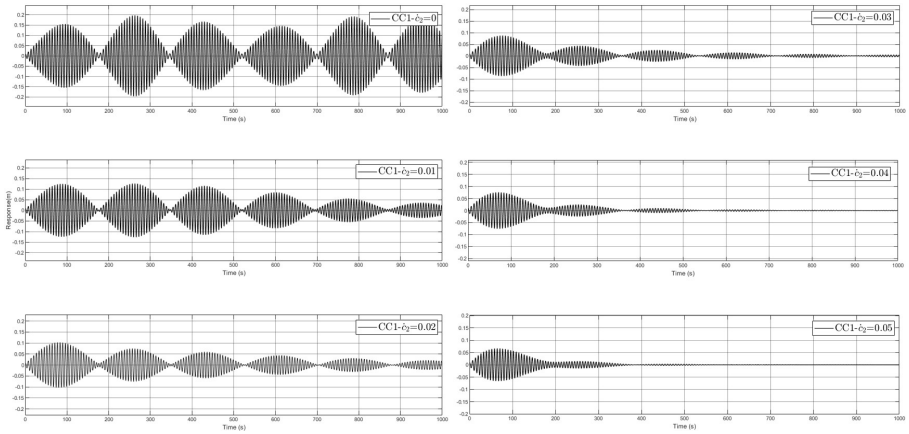

Figure 10 The in-plane response of the cable with different damping

It is clear from Figure 10, that the damping act positively in vibration control of the in-plane response. The larger the damping coefficient, the greater the restriction on the cable in-plane vibration. This is a common conclusion in most relative Refs (K. Zhan and W. X. Zhong, 1998) (Zhang Yan, Wang Huailei, and Yang Jie, 2010). However, the influence

effect in the dynamic system is complicated enough that the resonant cable may be affected by the damping of other components through the boundary conditions, as shown in Figure 11.

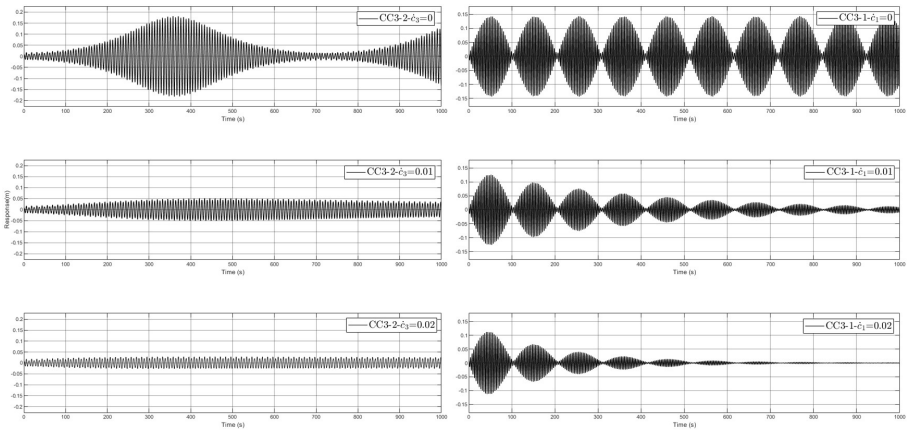

Figure 11 The in-plane response of the cable with different damping of the tower or the beam

The damping from other components does affect the in-plane vibration response of the cable through the energy conversion in the global system, while the effect of damping is positively correlated with the magnitude of the value. Due to the complexity of the cable-stayed bridge structure, the damping effect is actually an intensely complicated energy conversion process (X. Su, H. Kang, and T. Guo, 2022) (Z. X. Wang, B. Wang, and X. P. Chai, 2015) (Kang H J, Zhu H P, Zhao Y. Y. et al, 2005) (Nielsen S R K, Sichani M T, 2011).

Additionally, high-performance materials such as CFRP cables can be used instead of ordinary cables in engineering to avoid the threshold interval of the internal resonance conditions (K.H. Mei, S.J. Sun, X.Q. Li, G.Q. Jin, 2017). As known is that the unit quality of CFRP cable is only one-fourth of that of steel cable with the same rigidity conditions. To further discuss the effect of high strength and low weight cable materials on the resonance, the following compared case is applied:

Compared Case 5# (CC5): on the basic parameters of CC2 with no initial displacement applied, the external harmonic excitation from in-plane and out-of-plane are repectively applied to this dynamic system: $\omega_{u1} = \omega_{u1} = \kappa_{u1} = \kappa_{u2} = 1rad/s, \Psi_{u1} = \Psi_{w1} = 0.01m/s^2$. It is noticeable that the EA remains the same, which further illustrated that the value of Young's Module increases with the decrease of the mass and cross area. The variable value of damping is applied with the different unit mass of the cable. The variation trend is presented in Figure 12.

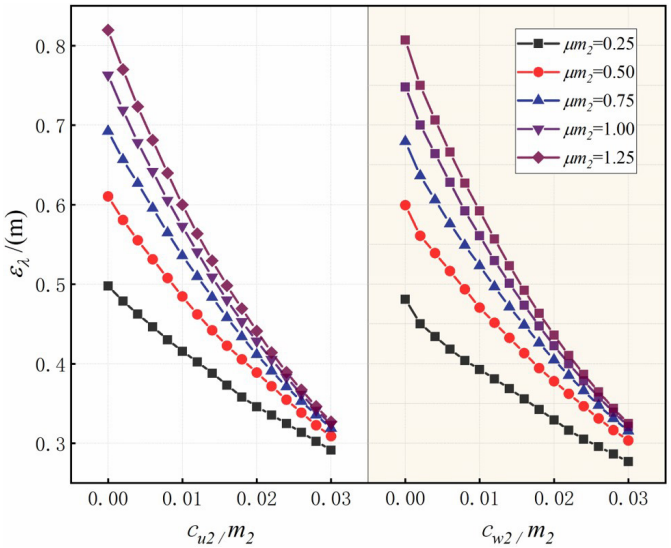

Figure 12 The trends under CC5

From Figure 12, it can be obtained that with the increase of the damping of in-plane and out-of-plane, the ε_u and ε_w also decrease gradually with almost the same reduction rate. In particular, the less mass of the cable, the smaller ε_λ of the vibration is under the same external harmonic excitation. It is illustrated that the increased damping ratio can

inhibit the occurrence of internal resonance or effectively reduce the ε_λ of the load plane when the internal resonance occurs.

5 Conclusion

Considering the non-linear geometric conditions, the dynamic behavior of in-plane and out-of-plane of a 3DOF model reduced from the tower-cable-beam structure is proposed, verified, and analyzed with analytical simulations in this paper. The dynamic model proposed in this paper can reduce a lot of the time of simulation compared to other models coupling nonlinear cables and the 3D FE model of the bridge has thousands of degrees of freedom. Through the systematical investigation and discussion, the following conclusions can be obtained:

(1) Through the analysis of the duration term in the dynamic equations, the internal resonance conditions of the dynamic system are obtained and verified by analytical simulation. It is worth noticing that the summation relationship between the component frequencies of in-plane and out-of-plane vibration is proved to be one of the conditions of out-of-plane internal resonance in the dynamic system, which further reveal some hard-explained phenomena in experimental investigations.

(2) Through the parametric analysis of the in-plane and out-of-plane internal resonance, it can be obtained that the mass ratio would affect ε_λ while the initial cable force and the tensile stiffness of the cable have little effect on the resonance strength. The smaller the mass ratio of cable-beam, the greater the cable resonance intensity.

(3) There is no mutual interference between the in-plane and out-plane resonances, and the external excitation in the axial direction of the cable would not lead to the internal resonance of the system. Thus, only out-of-plane resonance would occur under the internal resonance condition of the summation relationship.

(4) The effect of damping and high-strength cable on vibration control is relatively discussed in this paper. On one hand, the damping or the excitations of other components does affect the response of the cable, limited studies in this paper have already verified the effectiveness of the model for simulating the resonance process of the cable dynamic structure. On the other hand, under the same external excitation, ε_λ of the high-strength cable is smaller. Thus, the application of high-strength materials in engineering has a certain prospect for the internal vibration control of the cable.

(5) The non-linear properties of the parametric resonance should be in-depth investigated through the more refined model in the next-step investigations.

Data Availability: The data of this study are available from the corresponding author upon request.

Acknowledgements

Financial supports from Natural Science Foundation of Shaanxi Province. (no. 2021JQ-377) and Fundamental Research Business Fees of Central Universities of Chang'an Uni-versity (no. 310821161012) are gratefully acknowledged.

Author's Contribuitions: Conceptualization, K.C.; methodology, Y.L., K.W.; software, K.C., K.W.; formal analysis, K.C.; investigation, K.C.; resources, K.C. and Y.L.; writing—original draft preparation, K.C., K.W.; writing—review and editing, Y.L.; funding acquisition, Y.L. All authors have read and agreed to the published version of the manuscript.

Editor: Rogério José Marczak

References

Ming H W, Yi Q X, Hai T L, et al. (2014). Nonlinear responses of a cable-beam coupled system under parametric and external excitations. Archive of Applied Mechanics 84(2):173-185.

Main, J. A. and Jones, N. P. (1999). Full-scale measurements of stay cable vibration. In Proceedings of the 10th International Conference on Wind Engineering (10ICWE). Wind Engineering into the 21st century 1-3:963-970.

Tabatabai, Habib, and Armin B. Mehrabi, (1999). Vibration suppression measures for stay cables. In Proceedings of 17th International Modal Analysis Conference, Society for Experimental Mechanics 2:1237–1243.

Benedettini F, Rega G, (1987). Non-linear dynamics of an elastic cable under planar excitation. International Journal of Non-Linear Mechanics 2(6):497-509.

Fujino Y, Warnitchai P,and Pacheco B M (1993). Experimental and analytical study of autoparametric resonance in a 3DOF model of cable-stayed-beam. Nonlinear Dynamics 4(2):111-138.

Virlogeux M. (1998). Cable vibrations in cable-stayed bridges. Bridge Aerodynamic: 213-233.

K. Zhan and W. X. Zhong, (1998). Numerical study on parametric resonance of cables in cable stayed bridges. China Civil Engineering Journal 31(4):14–22.

Y. Zhang, H. Wang, and J. Yang, (2010). Dynamics of a three degrees of freedom nonlinear vibration model of cables and bridge decks and towers with the frequency 1:2:1 internal resonance. Journal of Dynamics and Control 8(1):62–66.

Yu Yanlei, Gao WeiCheng, Sun Yi, (2010). Study on refined model of stay cable parameters and its influencing factors. Engineering Mechanics 27(s2):178-185.

S. S. Chen and B. N. Sun, (2003). Numerical study on nonlinear parametric vibration of coupled cables and bridge decks. China Civil Engineering Journal 36(4):70–75.

Zhang L N, Li F C, Wang X Y, et al. (2017). Theoretical and Numerical Analysis of 1:1 Main Parametric Resonance of Stayed Cable Considering Cable-Beam Coupling. Advances in Materials Science and Engineering 2017 (6949081):10.

Georgakis C T, Taylor C A, (2013). Nonlinear dynamics of cable stays. Part 1: sinusoidal cable support excitation. Journal of Sound and Vibration 281(3-5):537-564.

Georgakis C T, Taylor C A, (2005). Nonlinear dynamics of cable stays. Part 1: sinusoidal cable support excitation. Journal of Sound and Vibration 281(3-5):565-591.

Wang Feng, Peng Zhang, et al., (2018). Analysis on Pylon-cable-girder Coupled Vibration Model and Influence Considering Temperature Effect. Journal of Highway and Transportation Research 35(11):51–60.

G. Ricciardi and F. Saitta, (2008). A continuous vibration analysis model for cables with sag and bending stiffness. Engineering Structures 30(5):1459–1472.

Gattulli V, Lepidi M, (2003). Nonlinear interactions in the planar dynamics of cable-stayed beam. International Journal of Solids and Structures 40(18): 4729-47.

Wu Z, Wei J, (2019). Nonlinear Analysis of Spatial Cable of Long-Span Cable-Stayed Bridge considering Rigid Connection. KSCE Journal of Civil Engineering 23(5):2418-2157.

E. Caetano, A. Cunha, V. Gattulli, and M. Lepidi, (2008). Cable-deck dynamic interactions at the International Guadiana Bridge: on-site measurements and finite element modelling. Struc- tural Control and Health Monitoring 15(3):237–264.

M. H. El Ouni, N. Ben Kahla, and A. Preumont, (2012). Numerical and experimental dynamic analysis and control of a cable stayed bridge under parametric excitation. Engineering Structures 45:244–256.

C. Sun, Y. Zhao, J. Peng, et al., (2018). Multiple internal resonances and modal interaction processes of a cable-stayed bridge physical model subjected to an invariant single-excitation. Engineering Structures 172:938–955.

H. J. Kang, T. D. Guo, and Y. Y. Zhao, (2016). Review on nonlinear vibration and modeling of large span cable-stayed bridge. Chinese Journal of Reoretical and Applied Mechanics 48:519–535.

Kefan Chen, Shuanhai He, Yifan Song, Linming Wu, Kang Wang and Hanhao Zhang; The Numerical Analysis for Parametric Resonance of Multicable System considering Interaction between Adjacent Beam Portions, Hindawi Shock and Vibration. 2021, Article ID 6937794, 19 pages.

Menwer Attarakih, Mazen Abu-Khader, and Hans-Jörg Bart, (2013). Dynamic analysis and control of sieve tray gas absorption column using MATALB and SIMULINK. Applied Soft Computing 13:1152-1169.

X. Su, H. Kang, and T. Guo, (2022). Modelling and energy transfer in the coupled nonlinear response of a 1:1 internally resonant cable system with a tuned mass damper. Mechanical Systems and Signal Processing 162:108058.

Z. X. Wang, B. Wang, and X. P. Chai, (2015). Research Advancement of Damping Techniques for Stay Cables of Long Span Cable-Stayed Bridges. Bridge Construction 45:13–19.

Kang H J, Zhu H P, Zhao Y Y et al, (2005). In-plane non-linear dynamics of the stay cables. Nonlinear Dynamics 7 :1385–1395.

Nielsen S R K, Sichani M T, (2011). Stochastic and chaotic sub- and superharmonic response of shallow cables due to chord elongations. Probabilistic Engineering Mechanics 26:44-53.

K.H. Mei, S.J. Sun, X.Q. Li, G.Q. Jin.(2017). Property of mode-coupled Internal -resonance of CFRP cables. China J. Highw. Transp 30.

Appendix 1 - The relevant coefficients of corresponding polynomials

$$\kappa_{u1}{}^2=\frac{k_{u1}}{m_1}+\frac{T_0}{lm_1},\dot{c}_{u1}=\frac{c_{u1}}{m_1},\Gamma_{1,1}=\frac{EA}{2l^3m_1},\Gamma_{1,2}=-\frac{T_0}{lm_1},\Gamma_{1,3}=-\frac{3EA}{2l^3m_1},\Gamma_{1,4}=\frac{3EA}{2l^3m_1},\Gamma_{1,5}=-\frac{EA}{2l^3m_1},\Gamma_{1,6}=\frac{EA}{2l^3m_1},\Gamma_{1,7}=-\frac{EA}{2l^3m_1},\Gamma_{1,8}=-\frac{EA}{l^3m_1},\Gamma_{1,9}=\frac{EA}{l^3m_1},\Gamma_{1,10}=\frac{EA}{2l^3m_1},\Gamma_{1,11}=-\frac{EA}{2l^3m_1},\Psi_{u1}=\frac{\psi_{u1}}{m_1} \quad (A.1)$$

$$\kappa_{w1}{}^2=\frac{k_{w1}}{m_1}+\frac{T_0}{lm_1},\dot{c}_{w1}=\frac{c_{w1}}{m_1},\Pi_{1,1}=\frac{EA_1}{2l^3m_1},\Pi_{1,2}=-\frac{EA}{l^3m_1},\Pi_{1,3}=\frac{EA}{2l^3m_1},\Pi_{1,4}=\frac{EA}{2l^3m_1},\Pi_{1,5}=-\frac{T_0}{lm_1},\Pi_{1,6}=-\frac{EA}{2l^3m_1},\Pi_{1,7}=\frac{EA}{l^3m_1},\Pi_{1,8}=-\frac{EA}{2l^3m_1},\Pi_{1,9}=-\frac{3EA}{2l^3m_1},\Pi_{1,10}=\frac{3EA}{2l^3m_1},\Pi_{1,11}=-\frac{EA}{2l^3m_1},\Psi_{w1}=\frac{\psi_{w1}}{m_1} \quad (A.2)$$

$$\kappa_{u2}{}^2=\frac{2T_0}{lm_2},\dot{c}_{u2}=\frac{c_{u2}}{m_2},\Gamma_{2,1}=-\frac{T_0}{lm_2},\Gamma_{2,2}=-\frac{EA}{2l^3m_2},\Gamma_{2,3}=\frac{3EA}{2l^3m_2},\Gamma_{2,4}=-\frac{3EA}{2l^3m_2},\Gamma_{2,5}=\frac{EA}{l^3m_2},\Gamma_{2,6}=\frac{EA}{l^2m_2},\Gamma_{2,7}=\frac{EA}{2l^3m_2},\Gamma_{2,8}=-\frac{EA}{2l^3m_2},\Gamma_{2,9}=\frac{EA}{2l^3m_2},\Gamma_{2,10}=\frac{EA}{l^3m_2},\Gamma_{2,11}=-\frac{EA}{l^3m_2},\Gamma_{2,12}=-\frac{EA}{2l^3m_2},\Gamma_{2,13}=\frac{EA}{l^3m_2},\Gamma_{2,14}=-\frac{EA}{l^3m_2},\Gamma_{2,15}=\frac{EA}{2l^3m_2},\Psi_{u2}=\frac{\psi_{u2}}{m_2} \quad (A.3)$$

$$\kappa_{w2}{}^2=\frac{2T_0}{lm_2},\dot{c}_{w2}=\frac{c_{w2}}{m_2},\Pi_{2,1}=-\frac{T_0}{lm_2},\Pi_{2,2}=-\frac{EA}{2l^3m_2},\Pi_{2,3}=\frac{EA}{l^3m_2},\Pi_{2,4}=-\frac{EA}{2l^3m_2},\Pi_{2,5}=-\frac{EA}{2l^3m_2},\Pi_{2,6}=\frac{EA}{2l^3m_2},\Pi_{2,7}=-\frac{EA}{l^3m_2},\Pi_{2,8}=\frac{EA}{l^3m_2},\Pi_{2,9}=\frac{EA}{l^2m_2},\Pi_{2,10}=\frac{EA}{2l^3m_2},\Pi_{2,11}=\frac{3EA}{2l^3m_2},\Pi_{2,12}=-\frac{3EA}{2l^3m_2},\Pi_{2,13}=\frac{EA}{l^3m_2},\Pi_{2,14}=-\frac{T_0}{lm_2},\Pi_{2,15}=-\frac{EA}{2l^3m_2},\Pi_{2,16}=-\frac{EA}{l^2m_2},\Pi_{2,17}=-\frac{EA}{2l^3m_2}\Pi_{2,18}=-\frac{3EA}{2l^3m_2},\Pi_{2,19}=\frac{3EA}{2l^3m_2},\Pi_{2,20}=-\frac{EA}{2l^3m_2},\Psi_{w2}=\frac{\psi_{w2}}{m_2} \quad (A.4)$$

$$\kappa_{u3}{}^2=\frac{k_{u3}}{m_3}+\frac{EA}{lm_3},\dot{c}_{u3}=\frac{c_{u3}}{m_3},\Gamma_{3,1}=\frac{EA}{2l^2m_3},\Gamma_{3,2}=\frac{EA}{2l^2m_3},\Gamma_{3,3}=\frac{EA}{2l^2m_3},\Gamma_{3,4}=-\frac{EA}{l^2m_3},\Gamma_{3,5}=\frac{EA}{2l^2m_3},\Psi_{u3}=\frac{\psi_{u3}}{m_3} \quad (A.5)$$

$$\kappa_{w3}{}^2=\frac{k_{w3}}{m_3}-\frac{T_0}{lm_3},\dot{c}_{w3}=\frac{c_{w3}}{m_3},\Pi_{3,1}=\frac{T_0}{lm_3},\Pi_{3,2}=\frac{EA}{2l^3m_3},\Pi_{3,3}=\frac{EA}{l^2m_3},\Pi_{3,4}=\frac{EA}{2l^3m_3},\Pi_{3,5}=\frac{EA}{2l^3m_3},\Pi_{3,6}=-\frac{EA}{2l^3m_3},\Pi_{3,7}=-\frac{EA}{l^2m_3},\Pi_{3,8}=-\frac{EA}{2l^3m_3},\Pi_{3,9}=-\frac{3EA}{2l^3m_3},\Pi_{3,10}=\frac{3EA}{2l^3m_3},\Pi_{3,11}=-\frac{EA}{2l^3m_3},\Psi_{w3}=\frac{\psi_{w3}}{m_3} \quad (A.6)$$